

Resting-State Connectivity Biomarkers of Cognitive Performance and Social Function in Individuals With Schizophrenia Spectrum Disorder and Healthy Control Subjects

Joseph D. Viviano, Robert W. Buchanan, Navona Calarco, James M. Gold, George Foussias, Nikhil Bhagwat, Laura Stefanik, Colin Hawco, Pamela DeRosse, Miklos Argyelan, Jessica Turner, Sofia Chavez, Peter Kochunov, Peter Kingsley, Xiangzhi Zhou, Anil K. Malhotra, and Aristotle N. Voineskos, for the Social Processes Initiative in Neurobiology of the Schizophrenia(s) Group

ABSTRACT

BACKGROUND: Deficits in neurocognition and social cognition are drivers of reduced functioning in schizophrenia spectrum disorders, with potentially shared neurobiological underpinnings. Many studies have sought to identify brain-based biomarkers of these clinical variables using a priori dichotomies (e.g., good vs. poor cognition, deficit vs. nondeficit syndrome).

METHODS: We evaluated a fully data-driven approach to do the same by building and validating a brain connectivity-based biomarker of social cognitive and neurocognitive performance in a sample using resting-state and task-based functional magnetic resonance imaging ($n = 74$ healthy control participants, $n = 114$ persons with schizophrenia spectrum disorder, 188 total). We used canonical correlation analysis followed by clustering to identify a functional connectivity signature of normal and poor social cognitive and neurocognitive performance.

RESULTS: Persons with poor social cognitive and neurocognitive performance were differentiated from those with normal performance by greater resting-state connectivity in the mirror neuron and mentalizing systems. We validated our findings by showing that poor performers also scored lower on functional outcome measures not included in the original analysis and by demonstrating neuroanatomical differences between the normal and poorly performing groups. We used a support vector machine classifier to demonstrate that functional connectivity alone is enough to distinguish normal and poorly performing participants, and we replicated our findings in an independent sample ($n = 75$).

CONCLUSIONS: A brief functional magnetic resonance imaging scan may ultimately be useful in future studies aimed at characterizing long-term illness trajectories and treatments that target specific brain circuitry in those with impaired cognition and function

Keywords: Biomarker, Functional outcomes, Imaging, Machine learning, Resting-state fMRI, Schizophrenia

<https://doi.org/10.1016/j.biopsych.2018.03.013>

Social cognitive and neurocognitive (SC/NC) deficits are associated with real-world functioning impairment in individuals with schizophrenia spectrum disorders (SSDs): schizophrenia, schizoaffective disorder, or schizophreniform disorder. However, these deficits can range from mild to severe, and some individuals with an SSD perform just as well or even better than matched controls (1,2). Past attempts to understand SC/NC deficits through separation into subtypes [e.g., type 1 vs. type 2 (3), good vs. poor outcomes (4), deficit vs. nondeficit (5–9)] are based on clinical characterization rather than data-driven approaches. Additionally, while DSM-IV subtypes have demonstrated separable domains of

psychopathology in schizophrenia (negative symptomatology, psychosis, and disorganization) (10–16), they failed to produce distinct groups of SC/NC performers or help uncover biomarkers of reduced functioning (17). The variability in SC/NC function, social impairment, and brain circuitry among people with SSDs may explain why standard univariate or case-control approaches have not translated well to biomarker identification.

Data-driven approaches that group individuals into neurophysiological subtypes, or “biotypes,” have been applied to persons with psychosis and depression, producing novel subgroups with distinct biomarkers (18–20). These approaches

SEE COMMENTARY ON PAGE 629

can uncover distinct biological factors that give rise to overlapping clinical presentations in disease. In SSDs, intact SC/NC processes are important for real-world function, and deficits in these domains are predictive of one's ability to form or sustain relationships, one's probability of gaining and maintaining employment, and long-term outcomes (15,21–28). Social cognitive processes have recently emerged as particularly strong determinants of functional outcome (25,29,30), and studies have identified the frontoparietal, corticomedial, and temporoparietal (or “mirror neuron”) circuitry (31) as important for imitation, empathy, theory of mind, and perspective taking. Smaller functional magnetic resonance imaging (fMRI) studies have focused on case-control differences in these regions (32–39), and such differences have not clearly translated to real-world function.

We assessed the utility of resting-state and task-based functional connectivity, and task activations for two social fMRI tasks, for identifying biologically different groups with differences in SC/NC performance. We first aimed to identify the fMRI data type (comparing task activations and/or connectivity from the tasks and resting-state data) that produced biotype groupings with the largest differences in SC/NC performance between groups using canonical correlation analysis (CCA), followed by hierarchical clustering that grouped the participants into biotypes based on these brain features (19). We validated our findings by comparing the identified groups on symptom, functional outcome, and structural neuroimaging measures (subcortical volumes, cortical thickness, and diffusion-based white matter metrics) not included in the original biotyping. We also tested whether the biotype of held-out participants could be correctly identified by a support vector machine classifier (SVC) trained using fMRI features, similar to a diagnostic test, and ranked the utility of each fMRI input by SVC classification accuracy. As control analyses, we compared these accuracies with those from SVCs trained to distinguish participants with normal or poor SC/NC scores, and diagnosis (SSD cases vs. controls) using the same input fMRI data. We hypothesized that SVCs trained to distinguish biotypes (i.e., groups informed by neurobiology) would achieve higher scores on held-out participants than would classifiers

trained on cognitive score-based groups or diagnostic groups. We finally repeated our analyses in an independent sample.

METHODS AND MATERIALS

We analyzed participant data from the three-site Social Processes Initiative in Neurobiology of the Schizophrenia(s) study ($N = 188$, mean age \pm SD = 33.0 ± 10.2 years; participants with SSD = 114, mean age \pm SD = 34.3 ± 10.2 years; control subjects = 74, mean age \pm SD = 31.0 ± 10.1 years). Demographics are summarized in Table 1; see Supplemental Table S5 for demographics at each site split by diagnosis. See the Supplement for inclusion and exclusion criteria. All participants signed an informed consent agreement, and the study was approved by institutional ethics boards at all participating institutions. All participants completed multiple assessments out of the MRI scanner. SC/NC functioning was assessed via the Penn Emotion Recognition Task (40), Reading the Mind in the Eyes Test (41), Relationships Across Domains (42), the three scales from the Awareness of Social Inference Test Revised (43), and six neurocognitive domains of the Measurement and Treatment Research to Improve Cognition in Schizophrenia (MATRICS) Consensus Cognitive Battery (MCCB) (44). Social functioning and quality of life were assessed via the Birchwood Social Functioning Scale (45) and Quality of Life Scale (46). Psychiatric symptom burden was assessed via the Brief Psychiatric Rating Scale (47) and Scale for the Assessment of Negative Symptoms (48). Two additional measures of diminished emotional expression and poor motivation that were based on the Scale for the Assessment of Negative Symptoms were included, as they relate to functional outcomes in SSD (16,49). Extrapyramidal symptoms were assessed via the Simpson–Angus Scale (50), general medical burden via the Cumulative Illness Rating Scale for Geriatrics (51), and antipsychotic medication exposure via chlorpromazine equivalents (52,53).

All sites used weekly phantom scans to ensure the stability of the T1-weighted, diffusion tensor imaging-based, and functional magnetic resonance imaging-based sequences over time. At all sites, we implemented standardized operating

Table 1. Demographics From the Three Sites of Data Collection

	Site CAMH	Site MPRC	Site ZHH
Group, $n_{SSD}:n_{HC}$	44:29	43:26	27:19
Sex, $n_F:n_M$	27:46	20:49	23:23
Ethnicity, $n_{nh}:n_h$	65:7	66:3	34:11
Language, $n_{efl}:n_{esl}$	62:11	66:3	44:2
Marital Status, $n_m:n_d:n_s$	11:2:60	13:6:50	6:5:33
Special Education, $n_Y:n_N$	6:67	11:58	12:34
Age, Years, Mean \pm SD	27.81 \pm 7.70	36.20 \pm 10.67	34.42 \pm 9.04
Education, Years, Mean \pm SD	14.40 \pm 2.43	14.33 \pm 2.37	14.33 \pm 2.54
Mother's Education, Years, Mean \pm SD	14.28 \pm 2.93	14.36 \pm 2.80	14.31 \pm 3.30
Father's Education, Years, Mean \pm SD	15.02 \pm 3.38	14.56 \pm 2.67	13.89 \pm 3.49
Handedness (Left = 0, Right = 1), Mean \pm SD	0.65 \pm 0.49	0.63 \pm 0.41	0.55 \pm 0.62
IQ, Mean \pm SD	112.13 \pm 12.45	107.04 \pm 15.95	101.58 \pm 15.31

CAMH, Centre for Addiction and Mental Health; d, divorced; efl, English as a first language; esl, English as a second language; F, female; h, Hispanic; HC, healthy control; M, male; m, married; MPRC, Maryland Research Centre; N, no; nh, not Hispanic; s, single; SSD, schizophrenia spectrum disorder; Y, yes; ZHH, Zucker Hillside Hospital.

protocols to minimize intersite variance in how the data were collected and how the participants behaved. These protocols standardized the administration of all in- and out-of-scanner tasks. In addition, participants were trained on how to participate in all in-scanner tasks (including the resting-state scan) with minimal head motion. An in-scanner camera was also employed to monitor participant movement during all scans. Finally, prior to analysis, all scans were checked for sufficient quality by experienced research staff, making use of in-house developed quality control system and accompanying dashboard (<https://github.com/TIGRLab/datman>; <https://github.com/TIGRLab/dashboard>). Quality control involved both quantitative (e.g., framewise displacement, signal-to-noise measures) and qualitative (e.g., detecting “sufficiently bad” ghosting or blurring by eye) monitoring. Some results demonstrating intersite stability have been documented in two recently published articles (54,55).

We report participants who pass quality control after completing a T1-weighted and resting-state ($n = 164$) fMRI scan, imitate/observe ($n = 93$) task (56), and empathic accuracy ($n = 183$) task (57,58). All three data types were analyzed via connectivity analysis. The data from the two task acquisitions were also analyzed using a general linear model as previously described (56,59). All connectivity data were preprocessed with FreeSurfer (60), AFNI (61), and FSL (62), including steps to minimize the impact of head-motion artifact (i.e., nuisance parameter regression, removing high-motion timepoints, rejecting high-motion participants) (63–65). Both tasks also separately underwent standard task-based fMRI preprocessing. For connectivity analysis, the Pearson correlation between the mean time series from each region of interest (ROI) in a 268-region atlas was calculated for a total of 35,778 r values per participant. For task activations, the mean t statistic from each ROI was calculated for a total of 268 t values per participant. See the [Supplement](#) for details.

The biotype analysis grouped participants with similar brain connectivity and/or function in regions associated with the SC/NC variables (19). First, we found a low-dimensional representation of cognitively relevant brain connections and/or task activations (defined here by the 12 SC/NC variables) using CCA, which is then clustered (hierarchical clustering using Ward’s method) into groups of participants with similar brain connectivity and/or function in regions associated with the cognitive variable of interest. Group differences in brain connectivity and/or function between biotypes were calculated using false discovery rate (FDR) ($q_{\text{FDR}} = .05$) to visualize these regions. See the [Supplement](#) for details.

We ranked the utility of each fMRI input (resting state, imitate/observe, and empathic accuracy) and analysis method (connectivity vs. task activations) by comparing SC/NC scores between biotypes. We validated our biotypes by comparing functional outcome and symptom burden scores, which were not included in the original analysis. For all SC/NC comparisons, we conducted a series of t tests to contrast the mean score of each group after Z scoring against the controls. Functional outcome and symptom burden scores were Z -scored and analyzed using only SSDs. All tests were corrected for multiple comparisons using FDR ($q_{\text{FDR}} = .05$) (66). We further validated our biotypes using both FreeSurfer-derived cortical thickness and subcortical volumes (60), as

well as tract-based spatial statistics–derived fractional anisotropy (FA) and mean diffusivity (MD) (67). See the [Supplement](#) for details.

We assessed the relationship between the fMRI features and defined groups (biotypes, cognitive score–based, or diagnosis–based) by training a linear SVC (using 10-fold cross-validation) to predict the group of held-out participants (test set) using the fMRI features from a training set. Each column of the fMRI input matrix was Z -scored before training. For all classification analyses conducted with biotype groups, CCA and clustering were performed on the training set alone for each fold, to prevent any information sharing between the training and test set. The mean accuracy, recall, precision, $f1$, score (harmonic mean of precision and recall), and area under the curve (AUC) of the receiver operator characteristic were calculated across all folds. For all cognitive score–based group analyses, we split participants into normal and poorly performing groups based on a percentile split of the first principal component of the 12 SC/NC scores. We took diagnosis–prediction performance as baseline. See [Supplemental Figure S1](#) for an overview and the [Supplement](#) for details.

To rank the utility of the fMRI features, we compared their ability to split the sample into groups with large SC/NC score differences via the t scores computed comparing SC/NC scores between biotypes (we report the mean t statistic across the 12 SC/NC scores assessed between groups in each case) and their performance when used to train an SVC to predict the biotype of held-out participants via the mean test set AUC computed during cross-validation. Each biotype model must surpass baseline SC/NC score differences between diagnostic groups to be considered useful. While SC/NC score differences between biotypes are expected given that CCA selected fMRI features with a strong relationship to the SC/NC, the magnitude of the between-group differences should modulate depending on the strength of that relationship. We then attempted to replicate our main fMRI findings in an independent sample of 75 participants who completed the resting-state and imitate/observe tasks; see the [Supplement](#) for details.

The analysis code is packaged as a freely available tool, xbrain (www.github.com/josephdviviano/xbrain), and the follow-up scripts used to analyze the outputs of xbrain can be found at www.github.com/josephdviviano/biotype.

RESULTS

All connectivity-based biotype analyses (resting state, imitate/observe, and empathic accuracy) consistently found two biotypes in our sample: a normal and a poorly performing biotype (in terms of SC/NC performance). CCA found different low-dimensional representations of each fMRI type considered; therefore, biotype membership differed depending on the input fMRI data.

Defining biotype groups with resting-state connectivity identified a poorly performing biotype with significantly lower SC/NC scores than the normal biotype (mean t difference between biotypes = 7.4, all significant $q_{\text{FDR}} = .05$). The differences in SC/NC scores between biotypes found using resting-state data were greater than the SC/NC score differences found when comparing diagnostic groups in the same participants, as well as the SC/NC score differences found between

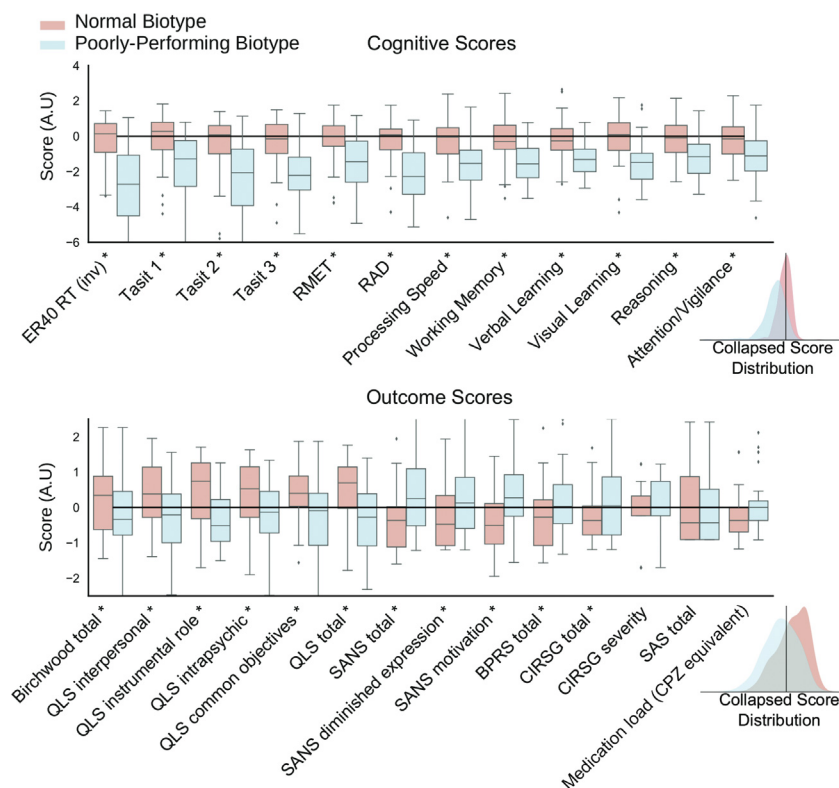


Figure 1. Cognitive scores and/or domains and outcome measures of biotypes based on resting-state functional connectivity. All cognitive scores were Z-scored against the mean of the scores from the healthy control group. All outcome scores were compared only among the patients and were therefore Z-scored within the group. Asterisks (*) denote significant differences after correcting for multiple comparisons with false discovery rate ($q_{FDR} = .05$). The poorly performing biotype group performed significantly worse on all cognitive scores and outcome measures tested. Members of this group also had higher general health symptom burden (as assessed by the Cumulative Illness Rating Scale for Geriatrics [CIRSG]). Insets for each graph show the probability density function of all Z-scored variables for each biotype to illustrate the overlap in cognitive scores and outcome variables between biotypes around $Z = 0$ (vertical black line). For this plot only, results of tests for which higher scores indicate higher impairment were inverted for visualization purposes. AU, arbitrary unit; BPRS, Brief Psychiatric Rating Scale; CPZ, chlorpromazine; ER40 RT (inv), Penn Emotion Recognition Task Inverted Emotion Recognition reaction time; RAD, Relationships Across Domains; RMET, Reading the Mind in the Eyes Test; QLS, Quality of Life Scale; SANS, Scale for the Assessment of Negative Symptoms; SAS, Simpson–Angus Scale; Tasit, Awareness of Social Inference Test.

the biotypes defined using all other functional MRI data (mean $t = 6.18$, all significant $q_{FDR} = .05$) (Figure 1 and Supplemental Figure S2; see the Supplement for replication and task details). While the poorly performing biotype's mean scores are lower, the distribution of their scores overlaps with those of the normally performing biotype around $Z = 0$. The poorly performing biotype that was defined using resting-state data consisted of 87% SSD cases ($n = 53$ of 61 individuals), and the normal biotype consisted of 41% SSD cases ($n = 42$ of 103 individuals) (Supplemental Figure S3). There was no significant difference in the proportions of participants by site in each biotype (see Table 2 for complete resting-state connectivity-based biotype demographics). The pattern observed for the 12 SC/NC scores included in the biotype procedure held for both the composite MATRICS score ($t_{164} = 9.45$, $p = 3.69 \times 10^{-17}$) and the number of correct responses from the Penn Emotion Recognition Task ($t_{164} = 5.93$, $p = 1.75 \times 10^{-8}$). Since these 12 SC/NC scores were used to define the biotypes in question, the test statistics were used only as an ordinal ranking measure to compare the utility of each input fMRI data type investigated.

Only the SSD cases from each biotype of the resting-state connectivity analyses were compared on functional outcome and burden scores ($n = 95$). SSD participants in the poorly performing biotype had significantly lower outcome scores as well as higher general health burden as measured by the Cumulative Illness Rating Scale for Geriatrics (Figure 1, Supplemental Table S1) compared with those of the normal biotype. Chlorpromazine equivalence comparisons revealed no significant

difference in medication load between biotypes. Compared with the normal biotype, the poorly performing biotype had smaller hippocampal, smaller nucleus accumbens, larger ventricles, and larger left globus pallidus volumes ($p \leq .017$); cortical thinning in the bilateral frontal and temporal cortex ($p \leq 8.04 \times 10^{-3}$), and greater MD in the bilateral external capsule, internal capsule, and fornix ($p \leq 4.95 \times 10^{-3}$). See the Supplement for details. In contrast to the biotypes found using resting state, those found using imitate/observe and empathic accuracy showed no significant differences when comparing functional outcome and symptom burden measures (data not shown). Structural validation analysis of the imitate/observe biotypes found cortical thickness differences in the left superior temporal sulcus ($p = 5.78 \times 10^{-4}$) and no other significant differences among subcortical volumes and FA/MD comparisons. Structural validation analysis of empathic accuracy biotypes found no significant differences among any of the structural measures considered.

The classification analyses where the goal was to predict biotype outperformed both cognitive score-based group prediction analyses and diagnosis-prediction analyses, as measured by mean AUC in the held-out participants (test set) across all 10 folds during cross-validation. Resting-state connectivity produced an accurate model for held-out participants (AUC = 0.88), outperforming most connectivity and task activations from both tasks (AUC = 0.39–0.86), with the exception of the imitate/observe task activations (AUC = 0.89). For prediction of cognitive score-based groups of either a 30th or 50th percentile cutoff, all analyses performed close to chance (AUC = 0.53–0.60), with the

Table 2. Demographics From the Resting-State Connectivity Biotypes

	Normal Biotype	Poorly Performing Biotype	Test Statistic	<i>p</i> (<i>q</i> _{FDR} = .05)
Site, <i>n</i> _{CAMH} : <i>n</i> _{MPRC} : <i>n</i> _{ZHH}	48:32:23	16:28:17	$\chi^2_2 = 6.86$	3.23×10^{-2}
Group, <i>n</i> _{SSD} : <i>n</i> _{HC}	42:61	53:8	$\chi^2_1 = 31.55$	1.93×10^{-8a}
Sex, <i>n</i> _F : <i>n</i> _M	41:62	17:44	$\chi^2_1 = 1.89$	1.69×10^{-8}
Ethnicity, <i>n</i> _{nh} : <i>n</i> _h	94:8	52:9	$\chi^2_1 = 1.28$	2.58×10^{-1}
Language, <i>n</i> _{eff} : <i>n</i> _{esl}	93:10	58:3	$\chi^2_1 = 0.64$	4.25×10^{-1}
Offspring, <i>n</i> _Y : <i>n</i> _N	11:92	12:48	$\chi^2_1 = 2.00$	1.57×10^{-1}
Marital Status, <i>n</i> _m : <i>n</i> _d : <i>n</i> _s	20:1:81	8:10:43	$\chi^2_2 = 14.77$	6.19×10^{-4a}
Special Education, <i>n</i> _Y : <i>n</i> _N	10:93	15:44	$\chi^2_1 = 5.95$	1.48×10^{-2a}
Age, Years, Mean \pm SD	29.66 \pm 8.90	36.43 \pm 10.01	$t_{162} = -4.36$	2.90×10^{-5a}
Illness Duration, Years, Mean \pm SD	7.61 \pm 6.3	16.32 \pm 10.63	$t_{93} = -4.6$	1.34×10^{-5a}
Education, Years, Mean \pm SD	15.11 \pm 2.12	13.05 \pm 2.25	$t_{162} = 5.74$	7.35×10^{-8a}
Mother's Education, Years, Mean \pm SD	14.60 \pm 2.92	13.86 \pm 2.94	$t_{162} = 1.46$	1.47×10^{-1}
Father's Education, Years, Mean \pm SD	14.92 \pm 3.36	13.88 \pm 2.94	$t_{162} = 1.94$	5.41×10^{-2}
Handedness (Left = 0; Right = 1), Mean \pm SD	0.61 \pm 0.50	0.67 \pm 0.47	$t_{162} = -0.77$	4.40×10^{-1}
IQ, Mean \pm SD	111.68 \pm 12.67	99.66 \pm 15.41	$t_{162} = 5.14$	1.19×10^{-6a}

CAMH, Centre for Addiction and Mental Health; d, divorced; eff, English as a first language; esl, English as a second language; F, female; FDR, false discovery rate; h, Hispanic; HC, healthy control; m, married; M, male; MPRC, Maryland Research Centre; N, no; nh, not Hispanic; s, single; SSD, schizophrenia spectrum disorder; Y, yes; ZHH, Zucker Hillside Hospital.

^aSignificant group differences after FDR correction (*q* = .05).

exception of resting-state connectivity (AUC = 0.64–0.67). Classification performance did not rely on the cutoff chosen as all score distributions overlapped between biotypes (Figure 1, Supplemental Figure S3). SVCs trained to distinguish biotypes outperformed SVCs trained to distinguish diagnosis in all cases. Only the SVC trained in resting-state connectivity predicted diagnosis well above chance (AUC = 0.74). The results from all classification experiments can be found in Table 3; see the Supplement for replication details and follow-up null experiments where either the class labels were randomized or the data were permuted before the CCA step (Supplemental Table S4).

Connectivity differences between resting-state biotypes show widespread differences in the brain's posterior regions (Figure 2). The normal biotype showed stronger whole-brain connectivity in ROIs associated with both the general cognition and reaction time networks (i.e., the thalamus and right superior temporal sulcus, which overlaps with the ventral attention network), while the poorly performing biotype shows stronger whole-brain connectivity in the occipital regions and ROIs associated with the somatomotor, mirror, and mentalizing networks, including the insula, inferior parietal lobule, postcentral gyrus, fusiform gyrus, and posterior cingulate. Most of the strongest group differences that replicated represented overconnectivity of the occipital and parietal regions with the rest of the brain, including the mirror network, in the poorly performing biotype (see the Supplement). Task connectivity group differences did not replicate (see the Supplement). Please see the Supplement for a comparison of quality control metrics on the TI-weighted, diffusion tensor imaging, and fMRI data.

DISCUSSION

Our data-driven approach found a poorly performing biotype of persons with SSDs and a normally performing biotype with respect to SC/NC performance. These fMRI features generalized to held-out participants: a linear SVC trained on brain

connectivity data alone accurately predicted the biotype of held-out scans. Comparisons of brain connectivity between the two biotypes revealed that the mirror and mentalizing regions are overconnected with the rest of the brain in the poorly performing biotype, and this result was replicated in a second, independent sample from a single site in the resting-state data. The normal biotype had an equal balance of healthy control participants and persons with an SSD, while the poorly performing biotype was almost entirely comprised of persons with an SSD. Validation using neuroanatomical analyses showed that the poorly performing biotype had lower cortical thickness, generally lower subcortical volumes, and higher white matter FA. Despite also testing task-based fMRI using well-established social brain tasks (empathic accuracy and imitate/observe), we found that resting-state connectivity was best able to distinguish biotypes with different SC/NC ability and real-world functional outcomes, while the task-based fMRI did less well and did not replicate in the independent sample.

Only the resting-state connectivity-based biotypes found a separation of the sample with SC/NC score differences greater than diagnosis (Supplemental Figure S1). Those in the poorly performing biotype demonstrated stronger functional connectivity between the occipital and parietal regions with the rest of the brain. These overconnected ROIs included the mirror network, a set of brain regions including the posterior superior temporal sulcus, anterior intraparietal sulcus, and the premotor cortex, which are engaged in both the perception of and the execution of biological motion (31,68). These regions replicated in an independent sample collected at one site (Figure 2). These mirror network regions are also believed to be important for both social cognition and empathy, and here we show that differences in mirror network brain organization are associated with poor functional outcomes and greater negative symptom burden. Furthermore, these groups showed significant differences in functional outcomes scores using the Birchwood Social Functioning Scale, which were not used to define the

Table 3. Classification Scores for Biotype, Cognitive Score Split, and Diagnosis Experiments

Analysis	Data	No. of Variables	AUC	Accuracy	Recall	Precision	f1
Biotype	REST connectivity	35,778	0.88 ± 0.03	0.81 ± 0.06	0.88 ± 0.03	0.83 ± 0.05	0.79 ± 0.07
Biotype	REST connectivity replication	35,778	0.83 ± 0.03	0.73 ± 0.06	0.83 ± 0.03	0.75 ± 0.05	0.71 ± 0.07
Biotype	IMOB GLM	268	0.89 ± 0.02	0.87 ± 0.03	0.89 ± 0.02	0.84 ± 0.04	0.83 ± 0.04
Biotype	IMOB connectivity	35,778	0.39 ± 0.16	0.77 ± 0.06	0.58 ± 0.11	0.68 ± 0.07	0.61 ± 0.09
Biotype	IMOB connectivity replication	35,778	0.62 ± 0.20	0.75 ± 0.11	0.67 ± 0.17	0.70 ± 0.12	0.67 ± 0.14
Biotype	EA GLM	268	0.60 ± 0.11	0.82 ± 0.05	0.72 ± 0.08	0.72 ± 0.06	0.71 ± 0.07
Biotype	EA connectivity	35,778	0.86 ± 0.02	0.78 ± 0.04	0.86 ± 0.02	0.77 ± 0.04	0.76 ± 0.05
Cog Split (50%)	REST connectivity	35,778	0.67 ± 0.03	0.67 ± 0.03	0.67 ± 0.03	0.68 ± 0.03	0.67 ± 0.03
Cog Split (50%)	IMOB GLM	268	0.56 ± 0.03	0.56 ± 0.03	0.56 ± 0.03	0.56 ± 0.03	0.55 ± 0.03
Cog Split (50%)	IMOB connectivity	35,778	0.56 ± 0.05	0.56 ± 0.05	0.56 ± 0.05	0.57 ± 0.06	0.56 ± 0.05
Cog Split (50%)	EA GLM	268	0.57 ± 0.04	0.57 ± 0.04	0.57 ± 0.04	0.58 ± 0.04	0.57 ± 0.04
Cog Split (50%)	EA connectivity	35,778	0.58 ± 0.03	0.58 ± 0.03	0.58 ± 0.03	0.58 ± 0.03	0.58 ± 0.03
Cog Split (30%)	REST connectivity	35,778	0.64 ± 0.04	0.61 ± 0.04	0.64 ± 0.04	0.62 ± 0.04	0.59 ± 0.04
Cog Split (30%)	IMOB GLM	268	0.49 ± 0.05	0.53 ± 0.04	0.49 ± 0.05	0.50 ± 0.04	0.49 ± 0.04
Cog Split (30%)	IMOB connectivity	35,778	0.60 ± 0.07	0.60 ± 0.07	0.60 ± 0.07	0.59 ± 0.06	0.57 ± 0.07
Cog Split (30%)	EA GLM	268	0.59 ± 0.03	0.59 ± 0.03	0.59 ± 0.03	0.58 ± 0.02	0.56 ± 0.03
Cog Split (30%)	EA connectivity	35,778	0.57 ± 0.04	0.57 ± 0.04	0.57 ± 0.04	0.56 ± 0.04	0.54 ± 0.04
Diagnosis	REST connectivity	35,778	0.74 ± 0.02	0.72 ± 0.02	0.74 ± 0.02	0.72 ± 0.02	0.72 ± 0.02
Diagnosis	IMOB GLM	268	0.49 ± 0.02	0.50 ± 0.02	0.49 ± 0.02	0.49 ± 0.02	0.49 ± 0.02
Diagnosis	IMOB connectivity	35,778	0.62 ± 0.04	0.61 ± 0.04	0.62 ± 0.04	0.62 ± 0.04	0.61 ± 0.04
Diagnosis	EA GLM	268	0.57 ± 0.03	0.58 ± 0.03	0.57 ± 0.03	0.57 ± 0.03	0.57 ± 0.03
Diagnosis	EA connectivity	35,778	0.52 ± 0.04	0.52 ± 0.04	0.52 ± 0.04	0.52 ± 0.04	0.52 ± 0.04

Each cell contains the mean and standard deviation test score over folds. The data column denotes which dataset was used to perform the experiment. For all biotype experiments, the same data type was used to biotype the participants and train the support vector machine classifier for classification. For all cognitive score split (cog split) experiments, the percentile used to split the first principal component of the 12 scores and/or domains is shown. This threshold defined the high- and low-scoring groups. For all diagnosis experiments, no social cognitive nor neurocognitive variables were used.

AUC, area under the curve; EA, empathic accuracy; GLM, generalized linear model; IMOB, imitate/observe task; REST, resting-state functional magnetic resonance imaging.

biotype groups. This finding suggests that the brain connectivity differences found in the poorly performing biotype derived from the resting-state data have real-world implications.

We performed a set of classification analyses to ensure that the fMRI features driving our biotype membership generalize to held-out participants. The resting-state biotype models outperformed all others considered in both the discovery and replication samples, and all biotype model-trained classifiers outperformed both classifiers trained via cognitive score-based groups (with the exception of the classifier trained using imitate/observe task activation-based biotypes) and classifiers trained via diagnosis-based groups. Therefore, we believe that our approach uncovered a distinct resting state-based biomarker that identifies a biologically distinct subset of participants. Our results also suggest that neurophysiological heterogeneity renders diagnostic group-based contrasts insufficient to detect the true disease-related brain organization variability. If a common functional brain organization gives rise to better and/or poorer cognitive performance, classifiers trained with cognitive score-based groups and biotypes would perform similarly: the classifier would simply learn to accurately associate the appropriate brain connectivity pattern with the appropriate cognitive group. This could not occur in our

sample owing to the clear overlap in the SC/NC score distributions between the poorest performers of the normal biotype and the strongest performers of the poorly performing biotype (Figure 1; Supplemental Table S1). Therefore, participants with similar scores can show different brain organizations (Figure 2).

The defining feature of the poorly performing biotype was overconnectivity between ROIs in the posterior and the rest of the brain. These results align with those of a recent study showing that the occipital and motor regions are over-connected in healthy control subjects with poorer cognitive scores and outcome measures (69), suggesting that this relationship is not specific to SSD. Occipital lobe abnormalities have been reported in schizophrenia (70,71), and abnormal connectivity of the occipital regions is associated with general risk of mental illness (72). As cortical development generally progresses from the posterior to the anterior cortex (73), this finding may be due to abnormal synaptic pruning associated with schizophrenia (74,75). The development of organized frontal activity in children and adolescents is dependent on the successful pruning of the parietal regions, including the mirror neuron network (76). Therefore, the poorly performing biotype might reflect those with halted or perturbed brain development at an earlier developmental stage. Alternatively,

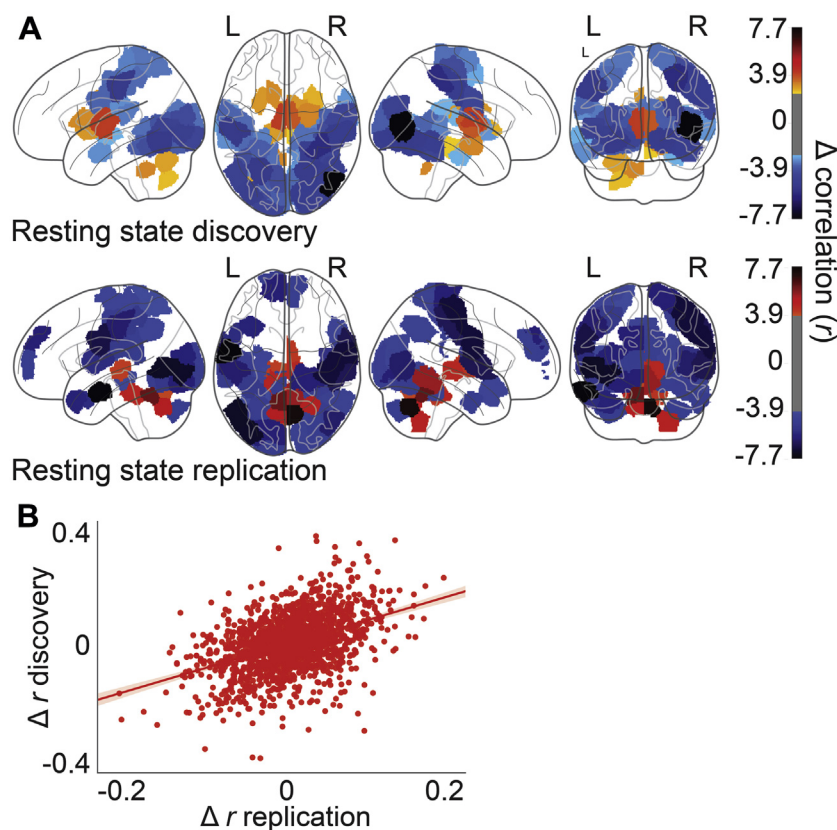


Figure 2. Resting-state connectivity differences between biotypes. In panel (A), the value in each region of interest (ROI) represents the difference of the summed connectivity values (r values) associated with that ROI between groups (normal vs. poorly performing biotype). The top 25% of all differences calculated between groups are shown. The contrast shows widespread differences along the frontal-posterior gradient. The normal group shows stronger connectivity emanating from general cognition and reaction time ROIs (red-orange), while the poorly performing biotype shows strong connectivity emanating from occipital and/or mirror ROIs (blues). Brain connections that were significantly different between biotypes in both samples (discovery and replication) are highly correlated ($r = .42$, $p < 1 \times 10^{-5}$ after 10,000 permutations), shown in panel (B). Specifically, this demonstrates that the pattern of connectivity differences between biotypes is similar in the two independent samples. L, left; R, right.

overconnectivity of the parietal and occipital regions may be viewed as compensatory organization, potentially in relation to aberrant development of frontal regions, which is a well-supported finding in schizophrenia (77).

Differences between the two biotypes using structural neuroimaging data in cortical thickness, subcortical volumes, and white matter FA, which were also not included in the original biotype model, lend validity to the replicated data-driven results, similar to a previously described approach (18). A number of studies have attempted (using almost exclusively structural neuroimaging approaches) to compare people with type 1 versus type 2 schizophrenia (3), poor versus good outcomes (4), or deficit versus nondeficit syndrome (5–9). These studies identified larger ventricles, gray matter differences, and more recently, white matter diffusion metric differences as potentially having the greatest effect size between groups. However, these approaches all require detailed and extensive clinical characterization, multiple assessments, and other time-intensive approaches. Our data-driven approach required only a short resting-state fMRI scan to reliably separate people with an SSD into two groups, one with poorer cognitive performance, greater negative symptom burden, and poorer functional outcome, and the other with performance more similar to that of the healthy control group.

Our finding that resting-state connectivity, and not task, data are best at isolating cognitively impaired participants with poor outcomes is in line with recent literature showing that subject-specific brain connectivity patterns at rest, but not

during tasks, allow for the reliable identification of individuals across scanning days (78) and across scanners (C. Hawco, Ph.D., *et al.*, unpublished data, August 2017). The two tasks considered (imitate/observe and empathic accuracy) grouped participants differently into the two biotypes (Supplemental Figure S6), and results were inconsistent between the discovery and replication sets. It is worth highlighting that the connectivity differences between biotypes for empathic accuracy were large when compared with both the imitate/observe and the resting-state data, suggesting that this task elicited robust brain connectivity related to task engagement. This measure of task engagement, however, does not seem to separate those with poor cognitive performance from the rest of the sample. We conclude that task fMRI activity better reflects task-specific brain activity than it does cognitive ability per se and consequently is less useful for deriving biologically different groups.

Our claim that the resting state is more useful than the tasks considered is limited because both tasks in our study involved the execution of motor commands in the scanner. Connectivity analysis is notoriously sensitive to motion (63). For both tasks, the removal of motion events may have had the unintended effect of removing task-related network activity or neurobiological information (79). Our ability to generalize these findings is limited by our use of closely matched scanning parameters and hardware, in addition to our extensive inclusion and exclusion criteria. Future work will require a larger sample of participants with varying clinical phenomenologies collected

on heterogeneous MRI configurations to train a classifier robust to these sources of variance. Our use of a cross-sectional sample leaves us unable to verify the stability of the biotypes over time; therefore, these results require longitudinal confirmation.

Site or scanner effects are typically sources of unwanted variance in connectivity studies, and they can drive spurious results. However, there was no significant difference in the number of participants in each biotype found (Table 2), and we replicated our findings in a second sample collected on a single scanner. While members of our resting-state poorly performing biotype group did show significantly worse general health as assessed by the Cumulative Illness Rating Scale for Geriatrics, they did not show significantly higher medication load as measured by chlorpromazine equivalence (Figure 1; Supplemental Table S1).

A fully trained model that distinguishes poor performers with specific alterations within their functional brain organization, such as the one discussed here, is a first step toward a biologically informed prognostic test that can be applied in the clinic to assess differences among patients that may be noted over a longer course of time in symptom burden, cognitive performance, and function. It may also have implications for treatment response. The model presented here generalizes to held-out participants and is demonstrated to work in an independent sample, suggesting strong external validity. This general approach may be useful for development of biologically driven tests for cognitive subtypes with divergent outcomes across psychiatric populations.

ACKNOWLEDGMENTS AND DISCLOSURES

This work was supported by the National Institute of Mental Health (Grant Nos. 1/3R01MH102324-01 to ANV, 2/3R01MH102313-01 to AKM, and 3/3R01MH102318-01 to RWB).

JDV and ANV had full access to all the data in the study and take responsibility for the integrity of the data and the accuracy of the data analysis.

Aside from the listed authors, we acknowledge the contributions of the remaining members of the Social Processes Initiative in Neurobiology of the Schizophrenia(s) (SPINS) group: Will Carpenter, Jen Zaranski, Eric Arbach, Sharon August, Gary Remington, Erin Dickie, Judy Kwan, Christina Plagiannakos, Mikko Mason, Marzena Boczulak, Dielle Miranda, Philipp Homan, Pamela DeRosse, Marco Iacoboni, and Michael Green.

We thank Christopher Honey, Erin Dickie, and Matthew Lovett-Barron for insightful discussions; Kristen Grimes, Leo Xu, Nicole Mackenzie, Rajeev Kareer, Joanna Collaton, Jessica D'Arcey, Shelley Grady, Adriana Halaby, Jef West, Rebecca Ruiz, John Fitzgerald, Kathryn Rhindress, Kristin Minara, Tracy A Giordonello, Lara Prizgint, Simran Kang, Taylor Marzouk, Sana Ali, Bernie Kompancaril, Christopher Morell, Danielle Beech, Darren Phane, George Nitzburg, Ivana De Lucia, and Natasha Bennett for performing behavioral and neuroimaging data collection; Nancy Lobaugh for managing and maintaining the consistency of the Centre for Addiction and Mental Health MRI equipment; and Steve Hawley, Jon Pipitone, Dawn Smith, and Tom Wright for data management.

AKM has served as a Consultant to Genomind, Concert Pharmaceuticals, and FORUM Pharmaceuticals. JG has consulted for Takeda, Lundbeck, and Hoffman–La Roche and receives royalty payments from the Brief Assessment of Cognition in Schizophrenia. RWB served on the advisory boards of Astellas Pharma; Avanir Pharmaceuticals; Boehringer Ingelheim RCV; Instrument Technologies, Inc.; Lundbeck; Roche; and Takeda. RWB has consulted for Takeda and Upsher-Smith Laboratories and served on the Data Safety Monitoring Board of Pfizer. GF has served on advisory boards for Hoffman–La Roche and Takeda and received speaker's fees from Hoffman–La Roche, Lundbeck, and Novartis. All other authors report no biomedical financial interests or potential conflicts of interest.

ARTICLE INFORMATION

From the Kimel Family Translational Imaging-Genetics Research Lab (JDV, NC, NB, LS, CH, ANV), Campbell Family Mental Health Institute, Centre for Addiction and Mental Health; the Department of Psychiatry (GF, CH, SC, ANV) and Institute of Biomaterials and Biomedical Engineering (NB), University of Toronto, and MRI Unit (SC), Research Imaging Centre, Centre for Addiction and Mental Health, Toronto, Ontario; Computational Brain Anatomy Laboratory (NB), Brain Imaging Center, Douglas Mental Health University Institute, Verdun, Quebec, Canada; Department of Psychiatry (RWB, JMG, PK), Maryland Psychiatric Research Center, Catonsville, Maryland; Department of Psychiatry (PD, MA, PK, XZ, AKM), The Donald and Barbara Zucker School of Medicine at Hofstra/Northwell, Hofstra University, Hempstead; Center for Psychiatric Neuroscience (PD, MA, PK, XZ, AKM), The Feinstein Institute for Medical Research, Manhasset; Division of Psychiatry Research (PD, MA, PK, XZ, AKM), The Zucker Hillside Hospital, Division of Northwell Health, Glen Oaks, New York; Department of Psychology (JT), Georgia State University, Atlanta, Georgia.

Address correspondence to Aristotle N. Voineskos, M.D., Ph.D., 250 College Street, Toronto, ON, M5T 1R8, Canada; E-mail: aristotle.voineskos@camh.ca.

Received Nov 22, 2017; revised Mar 12, 2018; accepted Mar 31, 2018.

Supplementary material cited in this article is available online at <https://doi.org/10.1016/j.biopsych.2018.03.013>.

REFERENCES

- Heinrichs RW, Miles AA, Smith D, Zargarian T, Vaz SM, Goldberg JO, Ammari N (2008): Cognitive, clinical, and functional characteristics of verbally superior schizophrenia patients. *Neuropsychology* 22:321–328.
- Muharib E, Heinrichs RW, Miles A, Pinnock F, Vaz SM, Ammari N (2014): Community outcome in cognitively normal schizophrenia patients. *J Int Neuropsychol Soc* 20:805–811.
- Crow TJ (1980): Molecular pathology of schizophrenia: More than one disease process? *Br Med J* 280:66–68.
- Mitelman SA, Torosjan Y, Newmark RE, Schneiderman JS, Chu K-W, Brickman AM, et al. (2007): Internal capsule, corpus callosum and long associative fibers in good and poor outcome schizophrenia: A diffusion tensor imaging survey. *Schizophr Res* 92:211–224.
- Buchanan RW, Breier A, Kirkpatrick B, Elkashef A, Munson RC, Gellad F, Carpenter WT (1993): Structural abnormalities in deficit and nondeficit schizophrenia. *Am J Psychiatry* 150:59–59.
- Rowland LM, Spieker EA, Francis A, Barker PB, Carpenter WT, Buchanan RW (2008): White matter alterations in deficit schizophrenia. *Neuropsychopharmacology* 34:1514–1522.
- Voineskos A, Foussias G, Lerch J, et al. (2013): Neuroimaging evidence for the deficit subtype of schizophrenia. *JAMA Psychiatry* 70:472–480.
- Fischer BA, Keller WR, Arango C, Pearlson GD, McMahon RP, Meyer WA, et al. (2012): Cortical structural abnormalities in deficit versus nondeficit schizophrenia. *Schizophr Res* 136:51–54.
- Wheeler AL, Wessa M, Szeszeko PR, Foussias G, Chakravarty MM, Lerch JP, et al. (2015): Further neuroimaging evidence for the deficit subtype of schizophrenia: A cortical connectomics analysis. *JAMA Psychiatry* 72:446–455.
- Buchanan RW, Strauss ME, Kirkpatrick B, Holstein C, Breier A, Carpenter WT (1994): Neuropsychological impairments in deficit vs nondeficit forms of schizophrenia. *Arch Gen Psychiatry* 51:804–811.
- Keefe RSE, Harvey PD, Lenzenweger MF, Davidson M, Apter SH, Schmeidler J, et al. (1992): Empirical assessment of the factorial structure of clinical symptoms in schizophrenia: Negative symptoms. *Psychiatry Res* 44:153–165.
- Kelley ME, van Kammen DP, Allen DN (1999): Empirical validation of primary negative symptoms: Independence from effects of medication and psychosis. *Am J Psychiatry* 156:406–411.
- Peralta V, Cuesta MJ (1995): Negative symptoms in schizophrenia: A confirmatory factor analysis of competing models. *Am J Psychiatry* 152:1450.

14. Sayers SL, Curran PJ, Mueser KT (1996): Factor structure and construct validity of the Scale for the Assessment of Negative Symptoms. *Psychol Assess* 8:269–280.
15. Strauss JS, Carpenter WT (1974): The prediction of outcome in schizophrenia: II. Relationships between predictor and outcome variables: A report from the WHO International Pilot Study of Schizophrenia. *Arch Gen Psychiatry* 31:37–42.
16. Strauss GP, Horan WP, Kirkpatrick B, Fischer BA, Keller WR, Miski P, *et al.* (2013): Deconstructing negative symptoms of schizophrenia: Avolition–apathy and diminished expression clusters predict clinical presentation and functional outcome. *J Psychiatr Res* 47:783–790.
17. Carpenter WT (2016): The RDoC controversy: Alternate paradigm or dominant paradigm? *Am J Psychiatry* 173:562–563.
18. Clementz BA, Sweeney JA, Hamm JP, Ivleva EI, Ethridge LE, Pearlson GD, *et al.* (2015): Identification of distinct psychosis biotypes using brain-based biomarkers. *Am J Psychiatry* 173:373–384.
19. Drysdale AT, Grosenick L, Downar J, Dunlop K, Mansouri F, Meng Y, *et al.* (2016): Resting-state connectivity biomarkers define neurophysiological subtypes of depression [published correction appears in *Nat Med* 2017 23:264]. *Nat Med* 23:28–38.
20. Hill SK, Reilly JL, Keefe RS, Gold JM, Bishop JR, Gershon ES, *et al.* (2013): Neuropsychological impairments in schizophrenia and psychotic bipolar disorder: Findings from the Bipolar-Schizophrenia Network on Intermediate Phenotypes (B-SNIP) study. *Am J Psychiatry* 170:1275–1284.
21. Brekke J, Kay DD, Lee KS, Green MF (2005): Biosocial pathways to functional outcome in schizophrenia. *Schizophr Res* 80:213–225.
22. Carpenter WT Jr, Kirkpatrick B (1988): The heterogeneity of the long-term course of schizophrenia. *Schizophr Bull* 14:645.
23. Combs DR, Waguspack J, Chapman D, Basso MR, Penn DL (2011): An examination of social cognition, neurocognition, and symptoms as predictors of social functioning in schizophrenia. *Schizophr Res* 128:177–178.
24. Couture SM, Penn DL, Roberts DL (2006): The functional significance of social cognition in schizophrenia: A review. *Schizophr Bull* 32:S44–S63.
25. Fett A-KJ, Maat A (2011): Social cognitive impairments and psychotic symptoms: What is the nature of their association? *Schizophr Bull* 39:77–85.
26. Grant C, Addington J, Addington D, Konner C (2001): Social functioning in first- and multipisode schizophrenia. *Can J Psychiatry* 46:746–749.
27. Green MF, Olivier B, Crawley JN, Penn DL, Silverstein S (2005): Social cognition in schizophrenia: Recommendations from the Measurement and Treatment Research to Improve Cognition in Schizophrenia New Approaches Conference. *Schizophr Bull* 31:882–887.
28. Green MF, Penn DL, Bental R, Carpenter WT, Gaebel W, Gur RC, *et al.* (2008): Social cognition in schizophrenia: An NIMH workshop on definitions, assessment, and research opportunities. *Schizophr Bull* 34:1211–1220.
29. Horan WP, Green MF, DeGroot M, Fiske A, Hellemann G, Kee K, *et al.* (2011): Social cognition in schizophrenia, Part 2: 12-month stability and prediction of functional outcome in first-episode patients. *Schizophr Bull* 38:865–872.
30. Savla GN, Vella L, Armstrong CC, Penn DL, Twamley EW (2012): Deficits in domains of social cognition in schizophrenia: A meta-analysis of the empirical evidence. *Schizophr Bull* 39:979–992.
31. Iacoboni M, Dapretto M (2006): The mirror neuron system and the consequences of its dysfunction. *Nat Rev Neurosci* 7:942–951.
32. Pinkham AE, Hopfinger JB, Pelphrey KA, Piven J, Penn DL (2008): Neural bases for impaired social cognition in schizophrenia and autism spectrum disorders. *Schizophr Res* 99:164–175.
33. Woodward ND, Rogers B, Heckers S (2011): Functional resting-state networks are differentially affected in schizophrenia. *Schizophr Res* 130:86–93.
34. Lee J, Quintana J, Nori P, Green MF (2011): Theory of mind in schizophrenia: Exploring neural mechanisms of belief attribution. *Soc Neurosci* 6:569–581.
35. Holt DJ, Cassidy BS, Andrews-Hanna JR, Lee SM, Coombs G, Goff DC, *et al.* (2011): An anterior-to-posterior shift in midline cortical activity in schizophrenia during self-reflection. *Biol Psychiatry* 69:415–423.
36. Skudlarski P, Jagannathan K, Anderson K, Stevens MC, Calhoun VD, Skudlarska BA, Pearlson G (2010): Brain connectivity is not only lower but different in schizophrenia: A combined anatomical and functional approach. *Biol Psychiatry* 68:61–69.
37. Garriy AG, Pearlson GD, McKiernan K, Lloyd D, Kiehl KA, Calhoun VD (2007): Aberrant “default mode” functional connectivity in schizophrenia. *Am J Psychiatry* 164:450–457.
38. Camchong J, MacDonald I, Angus W, Bell C, Mueller BA, Lim KO (2011): Altered functional and anatomical connectivity in schizophrenia. *Schizophr Bull* 37:640–650.
39. Swanson N, Eichele T, Pearlson G, Kiehl K, Yu Q, Calhoun VD (2011): Lateral differences in the default mode network in healthy controls and patients with schizophrenia. *Hum Brain Mapp* 32:654–664.
40. Kohler CG, Turner TH, Bilker WB, Brensinger CM, Siegel SJ, Kanes SJ, *et al.* (2003): Facial emotion recognition in schizophrenia: Intensity effects and error pattern. *Am J Psychiatry* 160:1768–1774.
41. Baron-Cohen S, Wheelwright S, Hill J, Raste Y, Plumb I (2001): The “Reading the Mind in the Eyes” test revised version: A study with normal adults, and adults with Asperger syndrome or high-functioning autism. *J Child Psychol Psychiatry* 42:241–251.
42. Sergi MJ, Fiske AP, Horan WP, Kern RS, Kee KS, Subotnik KL, *et al.* (2009): Development of a measure of relationship perception in schizophrenia. *Psychiatry Res* 166:54–62.
43. McDonald S, Flanagan S, Rollins J, Kinch J (2003): TASIT: A new clinical tool for assessing social perception after traumatic brain injury. *J Head Trauma Rehabil* 18:219–238.
44. Nuechterlein KH, Green MF, Kern RS, Baade LE, Barch DM, Cohen JD, *et al.* (2008): The MATRICS consensus cognitive battery, part 1: Test selection, reliability, and validity. *Am J Psychiatry* 165:203–213.
45. Birchwood M, Smith J, Cochrane R, Wetton S, Copestake S (1990): The Social Functioning Scale. The development and validation of a new scale of social adjustment for use in family intervention programmes with schizophrenic patients. *Br J Psychiatry* 157:853–859.
46. Heinrichs DW, Hanlon TE, Carpenter WT Jr (1984): The Quality of Life Scale: An instrument for rating the schizophrenic deficit syndrome. *Schizophr Bull* 10:388–398.
47. Overall JE, Gorham DR (1962): The Brief Psychiatric Rating Scale. *Psychol Rep* 10:799–812.
48. Andreasen NC (1989): Scale for the Assessment of Negative Symptoms (SANS). *Br J Psychiatry* 155:53–58.
49. Blanchard JJ, Cohen AS (2006): The structure of negative symptoms within schizophrenia: Implications for assessment. *Schizophr Bull* 32:238–245.
50. Simpson G, Angus J (1970): A rating scale for extrapyramidal side effects. *Acta Psychiatr Scand* 45:11–19.
51. Miller MD, Paradis CF, Houck PR, Mazumdar S, Stack JA, Rifai AH, *et al.* (1992): Rating chronic medical illness burden in geropsychiatric practice and research: Application of the Cumulative Illness Rating Scale. *Psychiatry Res* 41:237–248.
52. Lehman AF, Steinwachs DM (1998): Translating research into practice: The Schizophrenia Patient Outcomes Research Team (PORT) treatment recommendations. *Schizophr Bull* 24:1–10.
53. Rey M, Schulz P, Costa C, Dick P, Tissot R (1989): Guidelines for the dosage of neuroleptics. I: Chlorpromazine equivalents of orally administered neuroleptics. *Int Clin Psychopharmacol* 4:95–104.
54. Kochunov P, Dickie EW, Viviano JD, Turner J, Kingsley PB, Jahanshad N, *et al.* (2018): Integration of routine QA data into mega-analysis may improve quality and sensitivity of multisite diffusion tensor imaging studies. *Hum Brain Mapp* 39:1015–1023.
55. Chavez S, Viviano J, Zamyadi M, Kingsley PB, Kochunov P, Strother S, Voineskos A (2018): A novel DTI-QA tool: Automated metric extraction exploiting the sphericity of an agar filled phantom. *Magn Reson Imaging* 46:28–39.

56. Pfeifer JH, Iacoboni M, Mazziotta JC, Dapretto M (2008): Mirroring others' emotions relates to empathy and interpersonal competence in children. *Neuroimage* 39:2076–2085.
57. Kern RS, Penn DL, Lee J, Horan WP, Reise SP, Ochsner KN, *et al.* (2013): Adapting social neuroscience measures for schizophrenia clinical trials, Part 2: Trolling the depths of psychometric properties. *Schizophr Bull* 39:1201–1210.
58. Olbert CM, Penn DL, Kern RS, Lee J, Horan WP, Reise SP, *et al.* (2013): Adapting social neuroscience measures for schizophrenia Clinical Trials, Part 3: Fathoming external validity. *Schizophr Bull* 39:1211–1218.
59. Zaki J, Weber J, Bolger N, Ochsner K (2009): The neural bases of empathic accuracy. *Proc Natl Acad Sci U S A* 106:11382–11387.
60. Fischl B (2012): FreeSurfer. *Neuroimage* 62:774–781.
61. Cox RW (1996): AFNI: Software for analysis and visualization of functional magnetic resonance neuroimages. *Comput Biomed Res* 29:162–173.
62. Jenkinson M, Beckmann CF, Behrens TE, Woolrich MW, Smith SM (2012): FSL. *Neuroimage* 62:782–790.
63. Power JD, Barnes KA, Snyder AZ, Schlaggar BL, Petersen SE (2012): Spurious but systematic correlations in functional connectivity MRI networks arise from subject motion. *Neuroimage* 59:2142–2154.
64. Satterthwaite TD, Elliott MA, Gerraty RT, Ruparel K, Loughhead J, Calkins ME, *et al.* (2013): An improved framework for confound regression and filtering for control of motion artifact in the preprocessing of resting-state functional connectivity data. *Neuroimage* 64:240–256.
65. Van Dijk KR, Hedden T, Venkataraman A, Evans KC, Lazar SW, Buckner RL (2010): Intrinsic functional connectivity as a tool for human connectomics: Theory, properties, and optimization. *J Neurophysiol* 103:297–321.
66. Benjamini Y, Hochberg Y (1995): Controlling the false discovery rate: A practical and powerful approach to multiple testing. *J R Stat Soc Ser B Methodol* 57:289–300.
67. Smith SM, Jenkinson M, Johansen-Berg H, Rueckert D, Nichols TE, Mackay CE, *et al.* (2006): Tract-based spatial statistics: Voxelwise analysis of multi-subject diffusion data. *Neuroimage* 31:1487–1505.
68. Van Overwalle F, Baetens K (2009): Understanding others' actions and goals by mirror and mentalizing systems: A meta-analysis. *Neuroimage* 48:564–584.
69. Smith SM, Nichols TE, Vidaurre D, Winkler AM, Behrens TEJ, Glasser MF, *et al.* (2015): A positive-negative mode of population covariation links brain connectivity, demographics and behavior. *Nat Neurosci* 18:1565–1567.
70. Ardekani BA, Nierenberg J, Hoptman MJ, Javitt DC, Lim KO (2003): MRI study of white matter diffusion anisotropy in schizophrenia. *Neuroreport* 14:2025–2029.
71. Martínez A, Hillyard SA, Dias EC, Hagler DJ, Butler PD, Guilfoyle DN, *et al.* (2008): Magnocellular Pathway Impairment in Schizophrenia: Evidence from Functional Magnetic Resonance Imaging. *J Neurosci* 28:7492.
72. Elliott ML, Romer AL, Knodt AR, Hariri AR (2018): A connectome-wide functional signature of transdiagnostic risk for mental illness. *Biol Psychiatry* 84:452–459.
73. Gogtay N, Giedd JN, Lusk L, Hayashi KM, Greenstein D, Vaituzis AC, *et al.* (2004): Dynamic mapping of human cortical development during childhood through early adulthood. *Proc Natl Acad Sci U S A* 101:8174–8179.
74. Sekar A, Bialas AR, de Rivera H, Davis A, Hammond TR, Kamitaki N, *et al.* (2016): Schizophrenia risk from complex variation of complement component 4. *Nature* 530:177–183.
75. Keshavan MS, Anderson S, Pettergrew JW (1994): Is schizophrenia due to excessive synaptic pruning in the prefrontal cortex? The Feinberg hypothesis revisited. *J Psychiatr Res* 28:239–265.
76. Blakemore S, Choudhury S (2006): Development of the adolescent brain: Implications for executive function and social cognition. *J Child Psychol Psychiatry* 47:296–312.
77. Sakurai T, Gamo NJ, Hikida T, Kim S-H, Murai T, Tomoda T, Sawa A (2015): Converging models of schizophrenia – Network alterations of prefrontal cortex underlying cognitive impairments. *Prog Neurobiol* 134:178–201.
78. Finn ES, Shen X, Scheinost D, Rosenberg MD, Huang J, Chun MM, *et al.* (2015): Functional connectome fingerprinting: Identifying individuals using patterns of brain connectivity. *Nat Neurosci* 18:1664–1671.
79. Zeng L-L, Wang D, Fox MD, Sabuncu M, Hu D, Ge M, *et al.* (2014): Neurobiological basis of head motion in brain imaging. *Proc Natl Acad Sci U S A* 111:6058–6062.